Masuda *et al.*
Progress in Earth and Planetary Science (2023) 10:38
https://doi.org/10.1186/s40645-023-00571-1

Progress in Earth and Planetary Science

PAPER WITH FULL DATA ATTACHED

Open Access

Possible link between temperatures in the seashore and open ocean waters of Peru identified by using new seashore water data

Shuhei Masuda[1*], Masato Kobayashi[2], Luis Alfredo Icochea Salas[3] and Gandy Maria Rosales Quintana[3,4]

Abstract

The linkage between environmental conditions in the coastal ocean and the open sea varies greatly by region. It is important to clarify, on an area-by-area basis, what coastal monitoring information reveals about the open ocean and how much predictive information for the open ocean may be applicable to the coastal ocean. The Pacific Ocean off the coast of Peru is a monitoring area for the El Niño/La Niña, an oceanic–atmospheric phenomenon of global importance. However, there are not many reliable data along the Peruvian coast. We deployed a network of 6 logger sites along the Peruvian coast during 2017–2020 and compiled a useful, high-resolution dataset of water temperatures. We examined a possible link between temperatures in the coastal waters of Peru and the open sea by comparing the new dataset with historical temperatures in the open ocean. We confirmed that monthly mean anomalies of seashore water temperatures in coastal Peru were strongly correlated with those of open ocean sea surface temperatures. With one exception, the correlation coefficients ranged from 0.80 to 0.92 and were significant at $p < 0.01$. This result suggested that data obtained from monitoring along the Pacific coast of Peru could be used to indicate the state of the open ocean and that El Niño forecasts for the open ocean could be applied to coastal forecasting as well. Spectral analysis revealed that the periods of changes of seashore water temperature peaked at 80 and 120 days in the region north of 5° S. This result suggested that coastal monitoring might capture intraseasonal dynamics of equatorial Kelvin waves. The absence of clear peaks south of 5° S implied that equatorial wave energy did not penetrate far into off-equatorial regions along the Peruvian coast on intraseasonal timescales.

Keywords Climate change, Peruvian coast, Water temperature, Observation data

1 Introduction

The ocean plays a major role in climatic phenomena that occur on annual-to-decadal timescales. Among these phenomena are El Niño events, during which a 2–3 °C rise in sea surface temperature in the eastern tropical Pacific Ocean may induce major changes in atmospheric circulation that result in abnormal weather and natural disasters on a global scale (e.g., Kovats et al. 2003; Philander 2004). An accurate understanding of oceanic variability is therefore critical to elucidating and predicting medium- to long-term climate changes related to El Niño events.

Agriculture, fisheries, and other socioeconomic activities are concentrated in coastal regions. Numerous international programs launched since the end of the twentieth century have conducted intensive oceanographic observations to accurately understand oceanographic changes. Those efforts have included the World

*Correspondence:
Shuhei Masuda
smasuda@jamstec.go.jp
[1] Research Institute for Global Change, Japan Agency for Marine-Earth Science and Technology (JAMSTEC), Yokosuka, Japan
[2] Yokohama College of Commerce, Yokohama, Japan
[3] Department of Fisheries, Universidad Nacional Agraria La Molina, La Molina, Peru
[4] Department of Ocean Science, Tokyo University of Marine Science and Technology, Tokyo, Japan

Ocean Circulation Experiment (WOCE) and the global deployment of Argo floats to monitor a wide range of temperature and salinity changes in the ocean (e.g., Roemmich and Gilson 2009; Johnson et al. 2022). Tropical regions, in particular, have been intensively monitored to better understand the major global impacts of the El Niño/La Niña Southern Oscillation (ENSO) (e.g., McPhaden and Hayes 1989; McPhaden et al. 2019). However, climatic variations can differ greatly in the open ocean and in coastal environments (e.g., Santos et al. 2012).

Previous observational studies of tropical climate change have involved deployment of organized observation networks in the open ocean to capture phenomena on the scale of ocean basins. Most of the Argo float and moored-buoy arrays have been deployed west of the Galápagos Islands. Systematic oceanographic observations have been comparatively rare near the equatorial coast of South America (for instance, the NINO1+2 region bounded by 0°–10° S and 90°–80° W), which is an area closely associated with coastal influences of El Niño events and with the socioeconomic activities of Peru.

However, few coastal/seashore datasets have been organized or published thus far, and the study of coastal and open ocean links has been constrained by the paucity of relevant data. The technical difficulty of monitoring via remote sensing in coastal areas has also increased the value of publicly available in situ data.

In this study, we used autonomous logger instruments to monitor water temperatures along the Peruvian coast for three years to obtain for the first time systematic observations at strategic locations along the northern coast of Peru and to publish the data as an open dataset. This article is intended to describe the details of the observations we have made and the basic properties of the data. In addition, we describe interannual changes of water temperature in the seashore waters that were revealed by the data, and we discuss the relationships between these changes and corresponding changes in the open ocean. In addition, we use catch data to shed some light on the relationship between marine environmental conditions and catches.

2 Construction and Content

2.1 New in situ monitoring temperatures

Seashore water temperatures were continuously monitored from 2017 to 2020 at six locations along the coast of Peru using data loggers with built-in thermometers (automatic temperature measurement recorders, HOBO U22-001). These data loggers were installed at Mancora (4° 06′ S, 81° 04′ W), Cabo Blanco (4° 14′ S, 81° 13′ W), Talara (4° 34′ S, 81° 16′ W), Paita (5° 04′ S, 81° 08′ W; also known as Tierra Colorada), Chicama (7° 41′ S, 79° 26′ W), and La Punta in Callao (12° 04′ S, 77° 10′ W) (Fig. 1, Table 1). The spatial intervals ranged from 20 to 50 km between the first four of these loggers and around 500 km between Paita, Chicama, and Callao. The water temperatures at depths of approximately 2–8 m were acquired at 15-min intervals at each location. To ensure a continuous dataset, we replaced each logger every six months before the internal memory of the logger was filled. The sensors were calibrated using a thermostatic water bath at the Japan Agency for Marine-Earth Science and Technology.

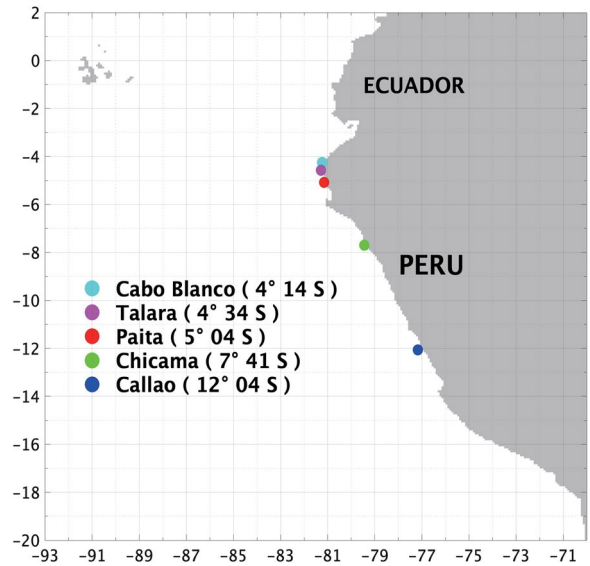

Fig. 1 Data logger locations. Map showing locations of data loggers deployed for this study in Peru (see Table 1)

Table 1 Logger and EN4 locations for study sites on the Peruvian coast

Pier Name and location	Logger location		EN4 location	
	Lat. (S)	Long. (W)	Lat. (S)	Long. (W)
Mancora	4° 06′	81° 04′	4°	81°
Cabo Blanco	4° 14′	81° 13′	4°	81°
Talara	4° 34′	81° 16′	5°	81°
Paita	5° 04′	81° 08′	5°	81°
Chicama	7° 41′	79° 26′	8°	79°
Callao	12° 04′	77° 10′	12°	77°

The data can be freely downloaded for use from https://www.jamstec.go.jp/goorc/data/peru_smasuda/. The data consist of six zip files, each of which contains approximately six months of logger data obtained from February 2017 to February 2020. Each folder contains files (TXT and MS Excel formats) named after the location where

the data were collected. The files contain the dates, times, sensor temperatures, and corrected temperatures.

2.2 Data used in analyses

2.2.1 Open-ocean observation datasets

We relied on quality-controlled subsurface ocean temperatures from the EN4.2.1.f.analysis.g10.201812 (EN4) dataset. We used temperatures at depths of 5.02 m and 207.4 m to represent temperatures at the surface and at a depth of 200 m, respectively. EN4 has been compiled by the Hadley Centre of the UK Meteorological Office (Good et al. 2013) and is based on the World Ocean Database 2009 (WOD09) along with Argo float data from the Argo Global Data Assembly Centers (GDACs) and quality-controlled, complementary data from the United States National Oceanographic Data Center compiled by the Arctic Synoptic Basin-wide Oceanography project and the Global Temperature and Salinity Profile Program. Details of the EN4 dataset have been summarized by Good et al. (2013) and references therein (e.g., Ingleby and Huddleston 2007; Gronell and Wijffels 2008; Guinehut et al. 2009). It should be noted that the logger data and EN4 dataset are completely independent; that is, the EN4 dataset does not contain any logger data and vice versa.

We identified variations of the 15 °C and 20 °C isotherms in the open ocean by using the National Oceanic and Atmospheric Administration (NOAA) daily subsurface temperature dataset from mooring buoys of the TAO/TRITON array at 0° N, 110° W (at depths of 1, 20, 40, 60, 80, 100, 120, 140, 180, 300, and 500 m) and 0° N, 95° W (at depths of 1, 5, 10, 15, 20, 25, 40, 45, 60, 80, 100, 120, 140, 180, 300, and 500 m).

2.2.2 Fisheries data

For comparison with the daily seawater temperature dataset, we obtained a dataset of daily anchovy landings from the Peruvian Sea Institute (IMARPE) from November 2019 to February 2020. Data were available only for Chicama and Callao.

Fishing vessels in Peru are classified as small artisanal vessels (capacity < 32.6 m^3), small-scale vessels (capacity < 32.6 m^3), and large-scale vessels (capacity > 32.6 m^3). Data were not available for the first class of vessels, which rely only on manual techniques. We estimated the total landing as the sum of the catch landed by small-scale and large-scale vessels.

3 Regional settings

Our study area is at the eastern edge of the equatorial Pacific, where the equatorial Kelvin waves involved in the development of El Niño events change their morphology (e.g., McPhaden and Yu 1999). The ocean conditions in this area are complex. Figure 2 shows the climatological distribution of sea surface temperature and two cross sections of subsurface water temperature compiled from the EN4 dataset. A two-layer structure is evident in this area. The main thermocline is on approximately the 15 °C isotherm, and upwelling occurs near the coast in response to the permanent easterly trade winds. This upwelling brings up nutrients from the deep sea to the surface and makes the coastal waters a rich fishing ground (e.g., Chavez et al. 1998; Chavez and Messié 2009; Qin et al. 2016; Espinoza-Morriberón et al. 2019). Under the influence of this structure of the water temperature and sea surface pressure, the current system consists of a deep eastward Equatorial Undercurrent and its subsurface branches (e.g., Lukas 1986; Johnson et al. 2002; Montes et al. 2010; Kuntz and Schrag 2018; Rosales Quintana et al. 2021) and surface currents that are dominated by an eastward Equatorial Countercurrent off the equator in the northern hemisphere and a westward South Equatorial Current in the southern hemisphere side. The subsurface Peru–Chile Undercurrent flows poleward along the coastline in the Southern Hemisphere. The equatorial waves that propagate with the El Niño/La Niña phenomenon transfer energy eastward in equatorial Kelvin waves (mostly changes in potential energy resulting from vertical movement of the main thermocline, e.g., Goddard and Philander 2000), transfer energy westward via equatorial Rossby waves, and transfer energy meridionally via coastal Kelvin waves that travel from the equatorial band to subtropical regions along the continental coastline.

4 Results and discussion

4.1 Monthly data features

Here we analyze how consistent the monthly averages of our new data were with existing open ocean data. We compiled separate datasets that consisted of monthly arithmetic average temperatures and daily mean temperatures. We applied a 48-h filter to the data to remove the diurnal tides before making the compilations (Thompson 1982).

The monthly average logger data feature interannual variability with amplitudes comparable to the typical annual variability, which exhibits a peak around 26 °C in February–March (Fig. 3a). The calibrated values of the water temperature tended to be higher closer to the equator; from north to south these were 23.5 ± 1.6 °C at Mancora, 21.1 ± 1.6 °C at Cabo Blanco, 20.0 ± 2.5 °C at Talara, 18.7 ± 2.8 °C at Paita, 17.3 ± 2.1 °C at Chicama, and 16.6 ± 1.4 °C at Callao. At Chicama and Callao, seasonal and spatial variations were relatively small.

The typical annual variability in the logger records consists of higher temperatures during austral summer

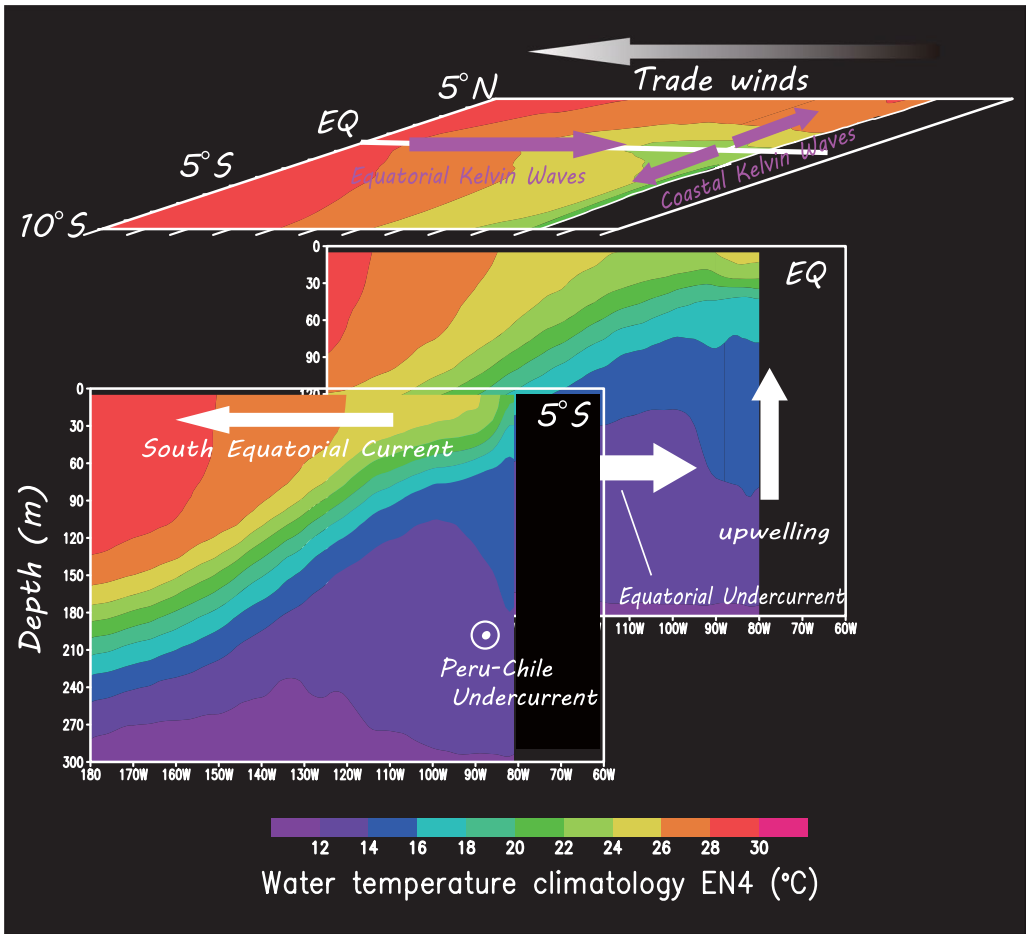

Fig. 2 Schematic view of the climatological ocean state off Peru. The distribution of sea surface temperature and cross sections of subsurface water temperature from the EN4 dataset during the period 2017–2020. The white arrows indicate major currents, and the magenta arrows denote oceanic waves related to ENSO energetics

(December–February) than during winter (June–August). This pattern is clearer in the four southernmost locations from Talara to Callao (4° S to 12° S), partly because they are farther from the variations of the Equatorial Front, which is generally located north of Paita (e.g., Fiedler and Talley 2006; Grados et al. 2018). The monthly anomalies from this seasonal pattern, expressed as standard deviations, were similar at the six sites: 0.8 °C for Mancora, 1.0 °C for Cabo Blanco, 1.1 °C for Talara, 1.5 °C for Paita, 1.5 °C for Chicama, and 0.9 °C for Callao (Fig. 3b). The average ratio of interannual to seasonal variation (anomaly values vs seasonal variation) of 0.79 indicates that the surface water temperature reflected almost equivalent forcings of the annual cycle and interannual variability.

The EN4 water temperatures and their anomalies for the locations nearest to the loggers (Table 1) are shown in Fig. 3c and d, respectively. It should be noted that the 1-degree spatial resolution of the EN4 dataset did not resolve some of the closely spaced logger points (Fig. 4). The water temperatures at the southernmost EN4 point, corresponding to Callao (12° S, 77° W), were lower than the temperatures at the rest of the EN4 points. Although the temperatures at the six loggers fluctuated around the same range of 16–28 °C, their means differed from those in the EN4 dataset, which were 21.1 °C at Mancora and Cabo Blanco (in the 4° S, 81° W cell), 20.6 °C at Talara and Paita (in the 5° S, 81° W cell), 20.8 °C at Chicama (in the 8° S, 79° W cell), and 19.6 °C at Callao (in the 12° S, 77° W cell). The standard deviations ranged between 2.6 and 3.0 °C.

Each temporal evolution of the EN4 dataset was similar to that of the logger data. The temperature anomalies from the seasonal cycle were 1.2 °C at Mancora and Cabo Blanco, 1.2 °C at Talara and Paita, 0.9 °C at Chicama, and 1.1 °C at Callao (Fig. 3d). The low average ratio of interannual to seasonal variations of the anomaly values (0.49) was due to the relatively large annual variations in the EN4 dataset. Because EN4 is an

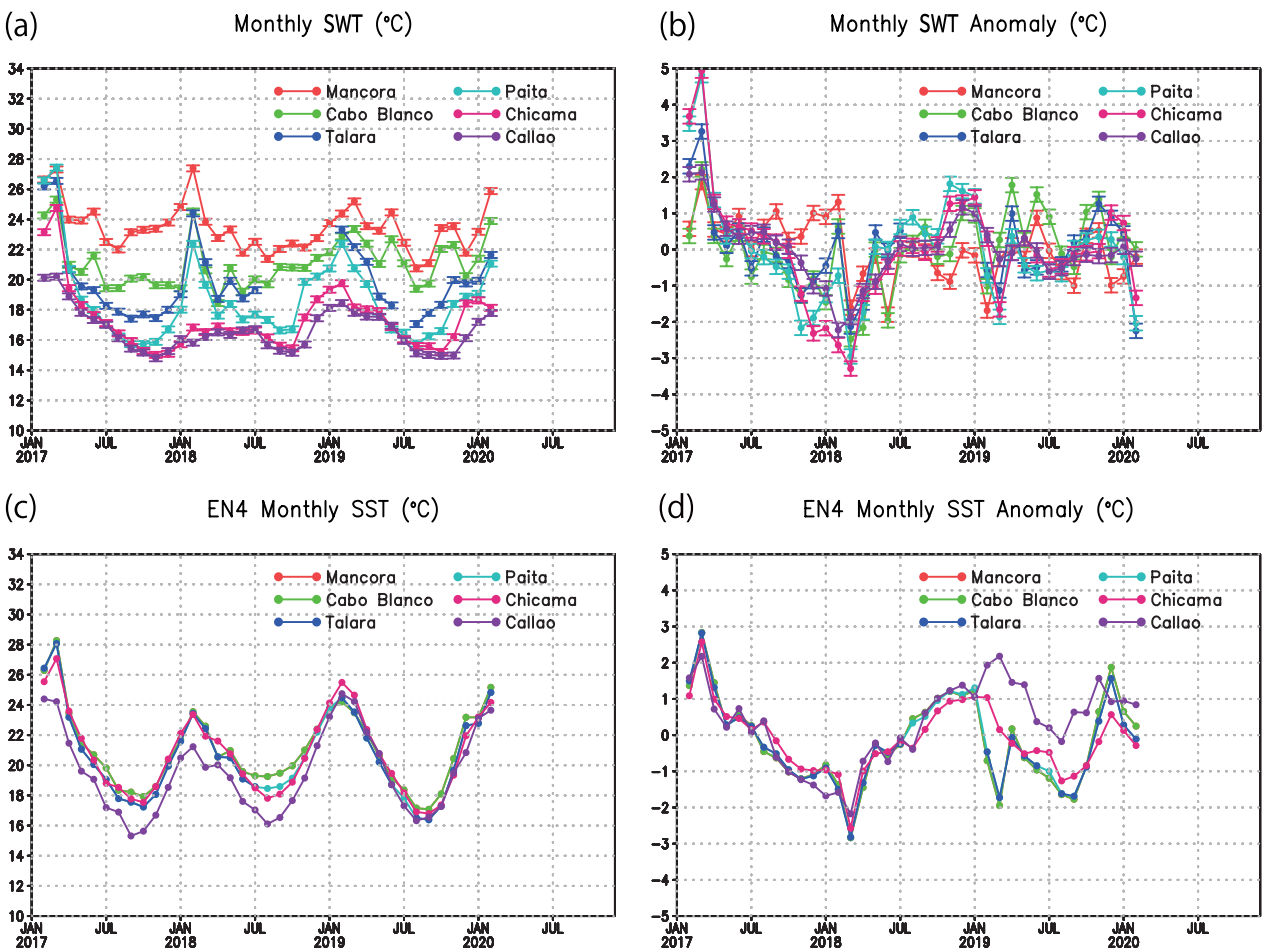

Fig. 3 Time series of monthly surface water temperature (SWT) at six sites along the Peruvian coast. **a** Calibrated seashore temperature from the loggers, **b** seashore temperature anomalies from logger data, **c** sea surface temperatures from the EN4 dataset, and **d** seashore temperature anomalies from the EN4 dataset

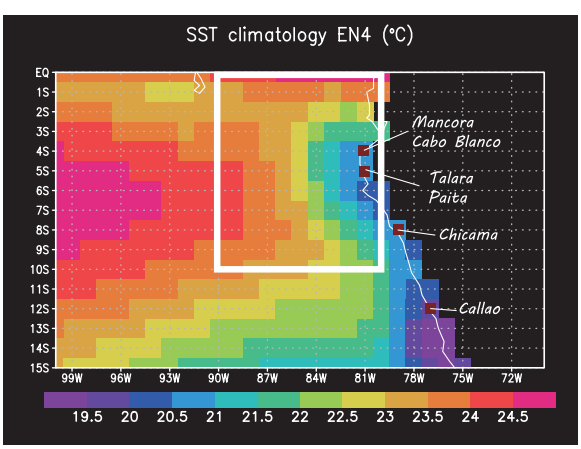

Fig. 4 Climatological sea surface temperature distribution. Map showing the climatological sea surface temperature distribution on the EN4 spatial grid at 1° resolution during 2017–2020. The white rectangle outlines the NINO1 + 2 region

integrated analysis dataset with one-degree grid cells, we infer that the seasonal component is somewhat accentuated in areas with sparse data.

The remainder of this analysis focuses on the anomaly values, which are plotted for each logger site in Fig. 5. There were strong correlations between EN4 and logger data for five of the six locations. The correlation coefficients ranged from 0.80 to 0.92 ($p < 0.01$). At Mancora, the northernmost site, the lack of statistical significance of the correlation coefficient of 0.26 ($p < 0.10$) was perhaps due to the fact that the highly variable interactions of the Equatorial Front off northern Peru are not well represented in EN4. For the other logger sites, the monthly average temperatures appeared to be well synchronized with the NINO1 + 2 sea surface temperature anomalies (Fig. 5g). It is interesting to note that the monthly anomalies of the logger data were also highly correlated with the coastal tide gauge data (0.77 at Talara and 0.70 at Callao, figures not shown). These

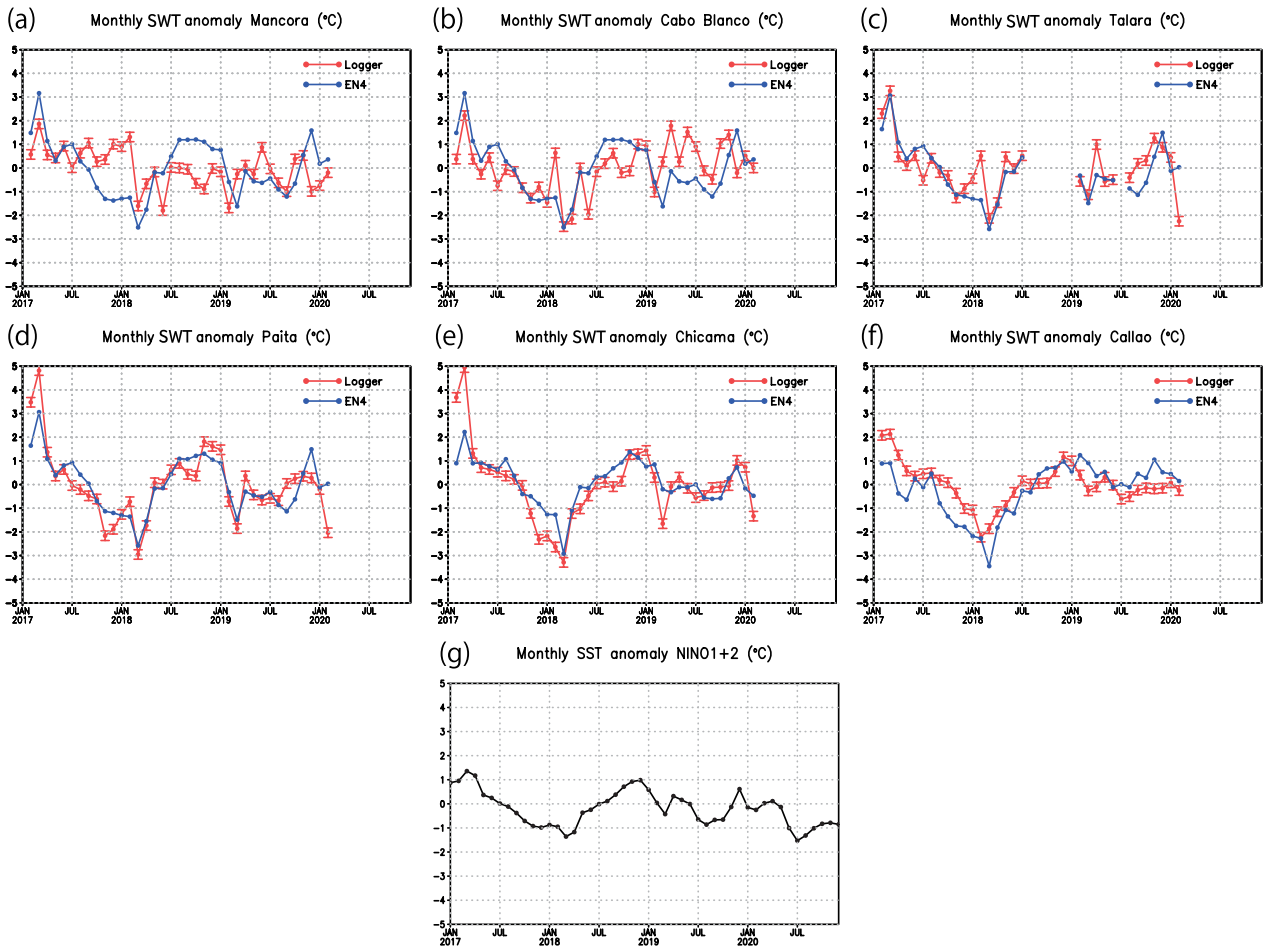

Fig. 5 Time series of monthly surface temperature anomalies. Anomalies at **a** Mancora, **b** Cabo Blanco, **c** Talara, **d** Paita, **e** Chicama, and **f** Callao. **g** NINO 1 + 2 sea surface temperature anomaly from EN4 dataset

results recall close link to the results of the previous researches (Clarke 1992; Jigena-Antelo et al. 2023).

We investigated the spatial correlation between the logger data and the EN4 dataset on a monthly and seasonal basis. We used only the northernmost (Cabo Blanco) and southernmost (Callao) logger sites to accommodate the coarser spatial resolution of the EN4 dataset.

The correlation diagram for the monthly surface temperature anomaly at Cabo Blanco shows the well-known El Niño spatial pattern (Fig. 6b). In the diagram for the subsurface (200-m depth), the fact that the area of strong correlation was more concentrated in the equatorial wave guide (Fig. 6e) reflects the strong influence of subsurface equatorial waves and the contribution of the Equatorial Undercurrent, which bifurcates in the Galápagos Islands and later feeds the Peru–Chile Undercurrent along the Peruvian coast (Montes et al. 2010; Rosales Quintana et al. 2021).

In the correlation diagram for the seasonal component, the surface temperature seemed to be determined by atmospheric forcing from solar insolation. The northern and southern hemispheres, as expected, were strongly differentiated (Fig. 6c). At a depth of 200 m, the much less distinct seasonal cycle reflected more complex causes (Fig. 6d). In sum, the variations of monthly surface temperature (Fig. 6a) reflected both subsurface equatorial wave dynamics and surface thermal forcing. The former tended to be subject to interannual fluctuations, whereas the latter was characterized by seasonal fluctuations. These patterns are by and large consistent with the fact that the ratio of interannual to seasonal variations ranged from 0.49 to 0.79 (vide supra). The spatial patterns of the subsurface temperatures and their anomalies were nearly identical (Fig. 6d and e).

The correlation diagrams for the Callao site were similar to those for Cabo Blanco, except that the patterns of monthly anomalies for surface and deep water exhibited a decay phase during El Niño (Fig. 7b and e). This finding was consistent with the propagation of coastal Kelvin waves from north to south and was corroborated by

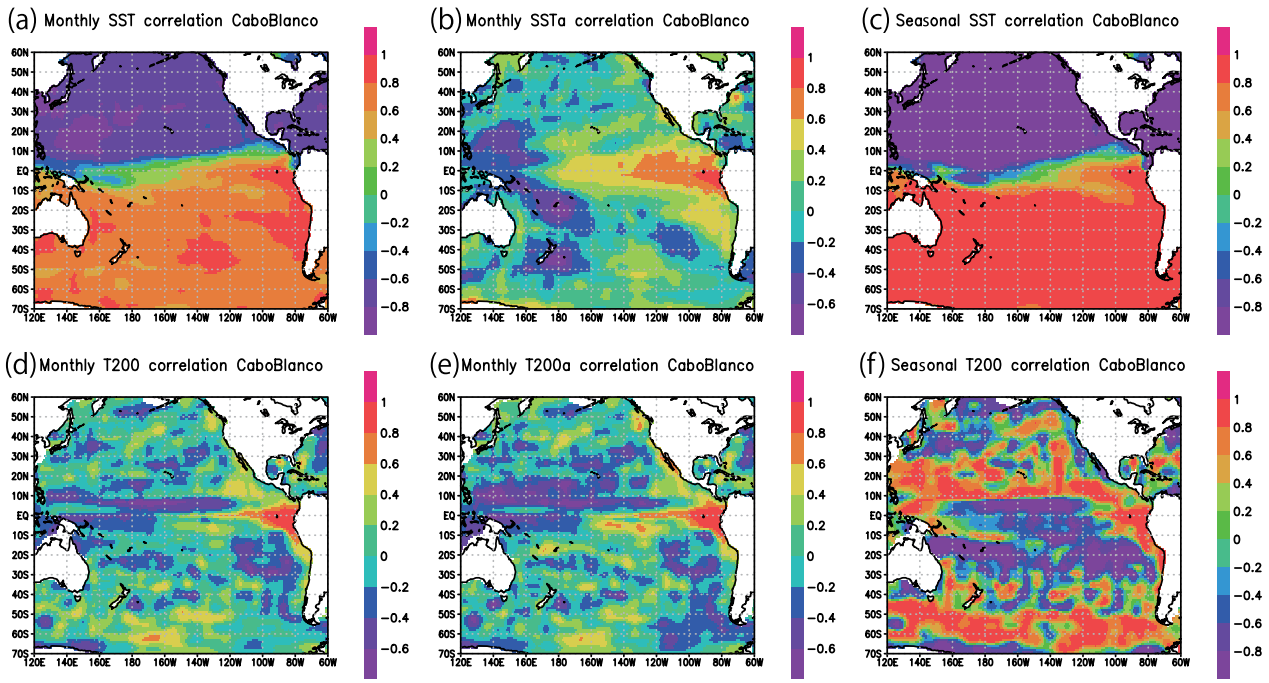

Fig. 6 Spatial correlation of the monthly water temperature. Maps showing spatial correlations (correlation coefficients) of monthly water temperature between Cabo Blanco (81° W, 4° S) and the Pacific basin from the EN4 dataset for 2010–2019 in relation to **a** surface temperatures, **b** surface anomalies, **c** surface seasonal cycle, **d** temperatures at 200 m depth, **e** anomalies at 200 m depth, and **f** seasonal cycle at 200 m depth

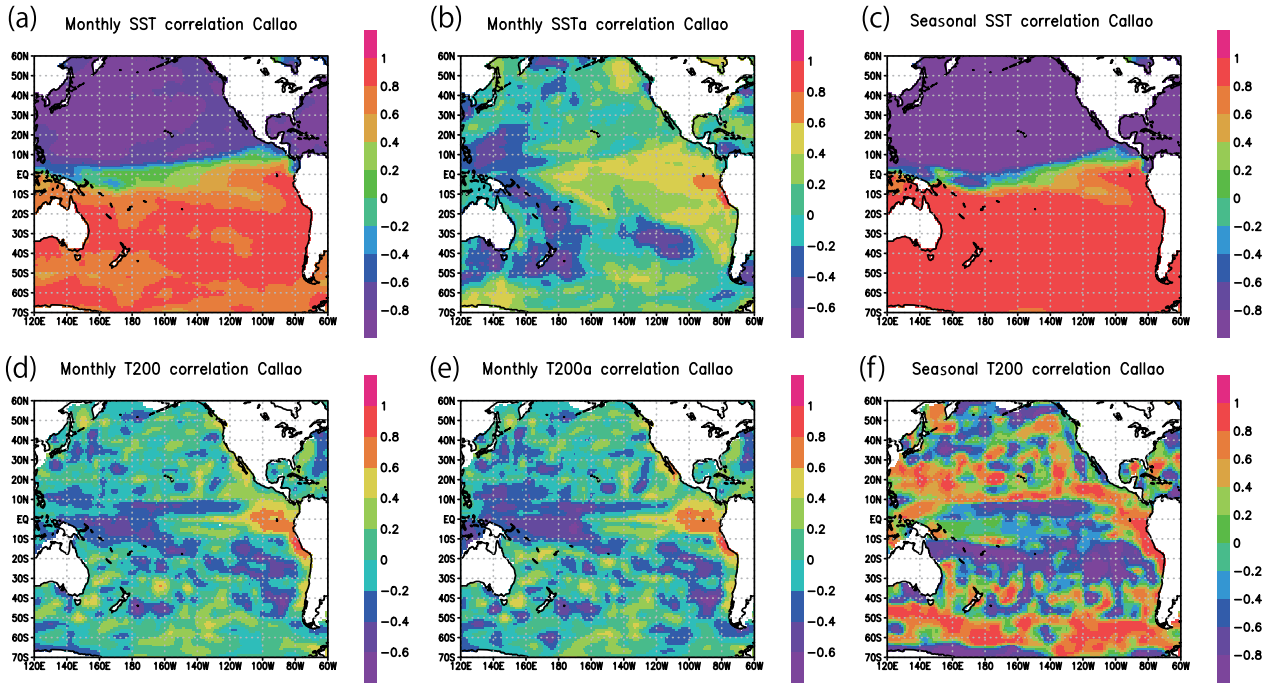

Fig. 7 Spatial correlation of the monthly water temperature. Same as Fig. 6 but for Callao (77° W, 12° S)

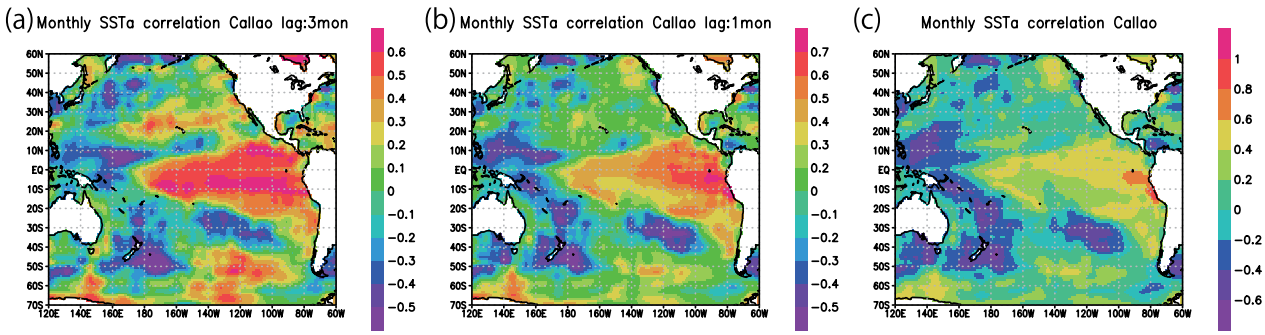

Fig. 8 Spatial lag correlation of the monthly water temperature. Same as Fig. 7b but for correlations with lags from Pacific basin data of **a** 3 months, **b** 1 month, and **c** 0 month (same as Fig. 7b)

diagrams incorporating a one- and three-month time lag that showed the well-known ENSO sequence (Fig. 8). The sea surface temperature anomaly in Callao led the distribution of SST anomalies shown in Fig. 8a and b by three months and one month, respectively. The implication is that sea surface variations in Callao can be partly traced back to equatorial Kelvin waves associated with ENSO events. Similarly, Rosales Quintana et al. (2021) have reported that the development of an anomalous flow of the Equatorial Undercurrent in the western Pacific (related to ENSO) may be detectable from the easternmost Pacific, where a strongly correlated signal can be detected between 30 and 35 days later in the Galápagos Islands.

Our results suggest that the monthly anomaly of the coastal surface temperature is dominated by El Niño. This scenario is consistent with the understanding from previous studies of this area, and the changes of water temperature obtained with the new observations were partly validated on the basis of monthly averages.

4.2 Daily data features

To demonstrate the utility of our data, we present here an analysis of daily average data. We applied a 48-h filter to the data to remove the signal from diurnal tides before making the daily compilations (Thompson 1982).

There are many possible sources of variation in daily mean temperature in the ocean, and our data alone cannot be used to identify the dynamics. However, we here attempt to make a comparison with equatorial waves as one of the possible causes. We subjected the daily mean temperature data from four of the six logger sites (Fig. 9) to a spectrum analysis. The results for the two northern sites, Mancora and Cabo Blanco, showed two clear peaks at periods of 80 and 120 days (Fig. 10). Those peaks had characteristics similar to those of the second and first baroclinic equatorial Kelvin waves with periods of 70 and 120 days, respectively, reported by Cravatte et al. (2003).

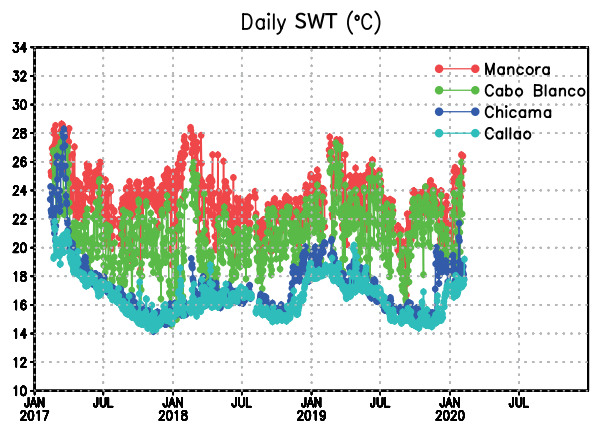

Fig. 9 Time series of daily seashore water temperatures at four Peruvian coastal sites

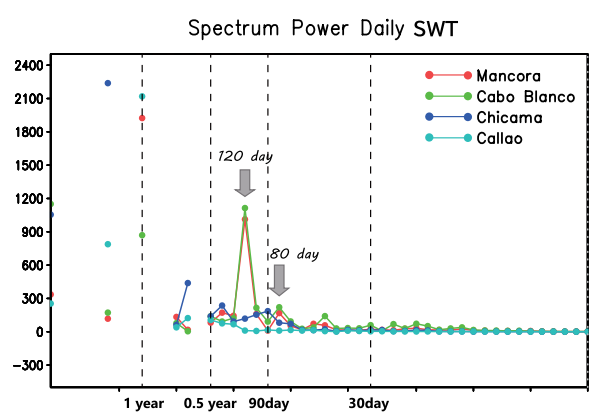

Fig. 10 Spectral analysis of the daily logger data shown in Fig. 9. Each color denotes Mancora, Cabo Blanco, Chicama, and Callao, respectively

The frequency shift from 70 to 80 days may be due to the different time periods analyzed by that study (the 1990s) and this one (e.g., Dewitte et al. 2008). However, the

cause of this shift should be addressed by comprehensive analysis using reanalysis data rather than by speculation.

In contrast, the data for Chicama and Callao did not show these peaks (Fig. 10). The implication of this discovery, that shorter-period equatorial waves may not leak beyond the equator, provides insight that may enhance understanding of the overall ENSO energy budget and the influences of ENSO on off-equatorial to mid-latitude oceanic changes.

4.3 Comparison with fisheries data

Coastal Kelvin waves and related changes in water properties can affect the principal fisheries in Peru through their influence on fish migration. Figure 11 shows anchovy landings along with daily temperature at the Paita, Chicama, and Callao piers. At the Paita pier (also known as the Tierra Colorada pier), water temperature rapidly increased by more than 6 °C (from 15.2 to 21.8 °C) from 13 to 18 November 2019. Although there are no catch data at this pier because the anchovy fleet did not operate near Paita, similar temperature changes occurred, with decreasing amplitude and a time lag of 5–8 days, at the two sites south of Paita that may have been related to coastal Kelvin waves. At the Chicama pier (350 km south of Paita), an abrupt increase of water temperature to about 20 °C began on 25 November, and the total daily anchovy catch drastically decreased from around 15,000 t to less than 3,000 t. The persistence of warm water temperatures until 17 January may has been related to reduced daily landings during that period. At the Callao pier (400 km south of Chicama), there was a small temperature increase that began on 28 November. The temperature reached 16.8 °C without a clearly related change in landings. The estimated speed of propagation of the signal was 0.51 m/s from Paita to Chicama and 1.15 m/s from Chicama to Callao. Because the speed of propagation of a coastal Kelvin wave would generally be around 0.4 m/s (Chelton and Davis 1982), a detailed assessment that took into account factors such as topography

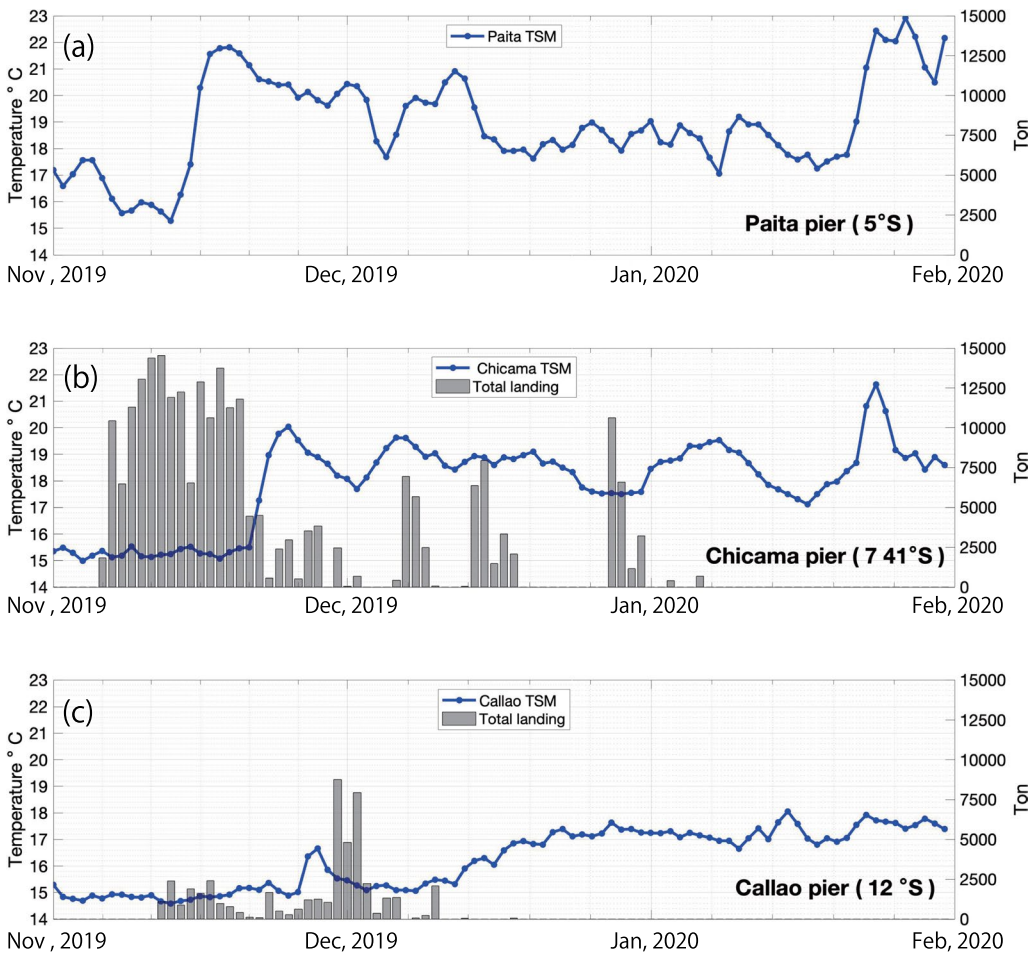

Fig. 11 Fishery data plot. Time series of daily anchovy landings and daily water temperatures at **a** Paita, **b** Chicama, and **c** Callao piers from November 2019 to February 2020

and stratification would be necessary to reveal the true nature of this "propagation".

It may be worth noting that an increase in the proportion of juveniles at the Callao pier started in January, when the fishing season was closed by the Peruvian authorities (IMARPE 2020). One cause of the abrupt increase of water temperature in November 2019 may have been the changes in the open ocean that were observed in the preceding months (Fig. 12). The subsurface water temperatures at 0° N, 110° W, and 0° N, 95° W reveal a deepening of the 15 °C and 20 °C isotherms that suggests the passage of a Kelvin wave in October 2019 that reached the Peruvian coast in November. It was first observed at 0° N, 110° W on 9 October and reached the

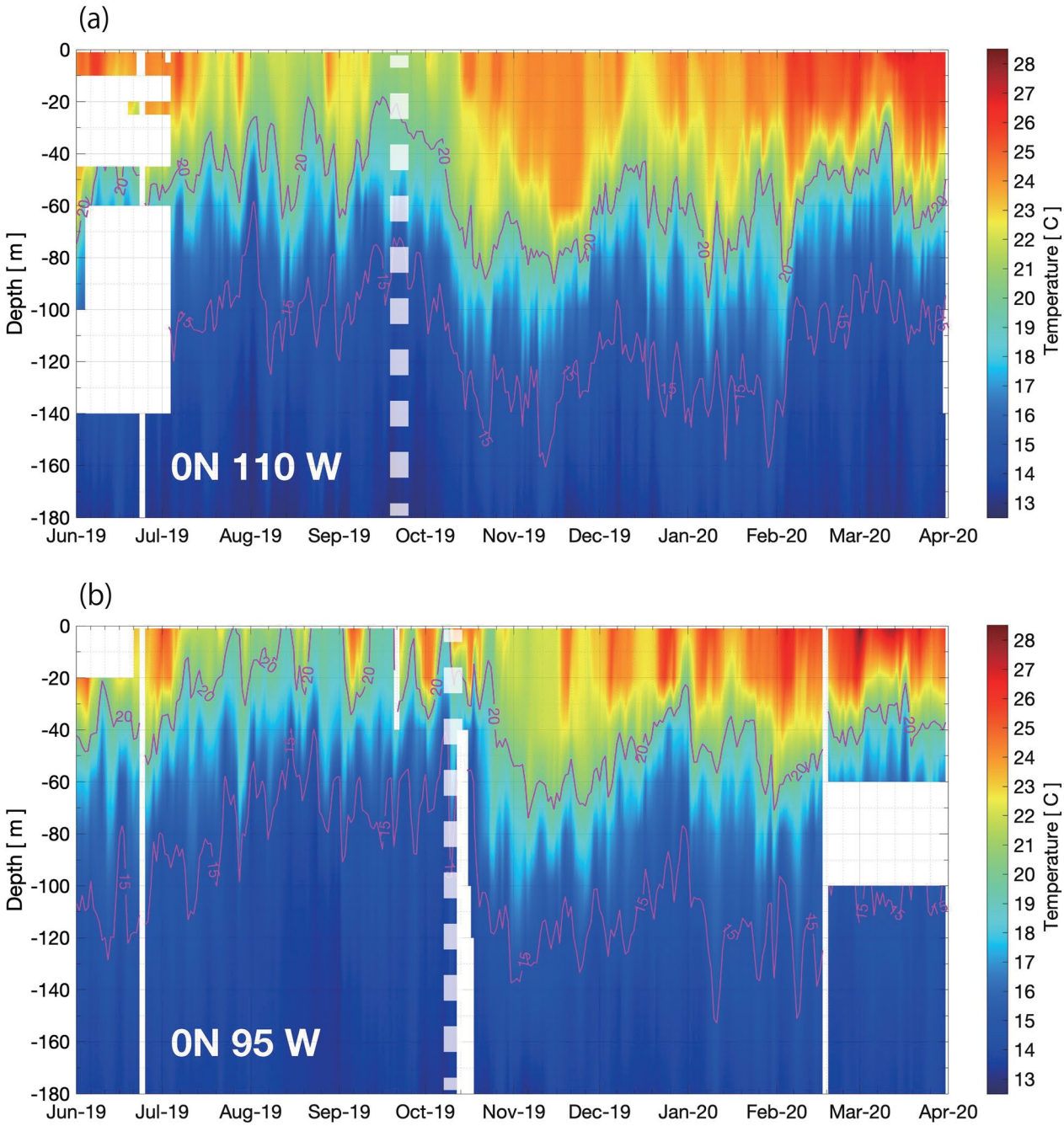

Fig. 12 NOAA Daily subsurface temperatures at **a** 0° N, 110° W and **b** 0° N, 95° W from June 2019 to March 2020. Magenta lines indicate the 15 °C and 20 °C isotherms. The white bars in (**a**) and (**b**) denote 9 October and 22 October, respectively

buoy at 0° N, 95° W on 22 October (white dashed bars in Fig. 12). Because this single example cannot be the basis for any firm conclusions, it will be increasingly necessary to acquire and publish data that can be used to accumulate such examples.

5 Conclusions

We installed new loggers to monitor seawater temperatures at six coastal sites in Peru from 2017 to 2020. The data are open and available in a well-organized, free dataset. This valuable dataset has resulted from high-resolution monitoring of Peruvian coastal waters.

Use of this dataset enabled us to confirm that coastal surface water temperatures were closely linked to monthly temperature anomalies and aspects of El Niño in the open ocean. The temperature anomalies at the southern coastal sites lagged those at northern coastal sites by about one month. This difference may be attributable to the passage of coastal Kelvin waves.

The high temporal resolution of our monitoring system may enable detection of equatorial Kelvin waves and shorter-term oceanic phenomena. The demonstration by our data that seashore water temperatures exhibited variability with periods of 80 and 120 days in the northern (equatorial) part of the study area suggests that equatorial waves may not penetrate far into higher latitudes on sub-seasonal timescales. Nevertheless, it is not possible to draw general conclusions from an analysis of a short period of only three years, when the cold ENSO phase was dominant.

There are many uncertainties in our knowledge of the area on the eastern boundary of the Pacific Ocean because of insufficient observation coverage. The kind of organized network of observations along the Peruvian coast described herein and publication of the reported data may greatly enhance that knowledge.

Abbreviations

ENSO	El Niño/La Niña Southern Oscillation
GDAC	Argo Global Data Assembly Centre
IMARPE	Peruvian Sea Institute
JAMSTEC	Japan Agency for Marine-Earth Science and Technology
NOAA	National Oceanic and Atmospheric Administration
WOCE	World Ocean Circulation Experiment
WOD09	World Ocean Database 2009

Acknowledgements

We are grateful to the National Fund for Fisheries Development (FONDEPES), the Hydrographic Department of the Peruvian Navy (DIHIDRONAV), the Peruvian Sea Institute, and Industrial Pesquera Santa Monica for permission to install data loggers inside their facilities. Our work benefited from support by Dr. H. Uchida with respect to calibration of the sensors we used. Numerical calculations were performed on the Data Analyzer of JAMSTEC.

Author contributions

SM conceived and designed the study. MK proposed the topic and carried out seashore observations. LAIS supported seashore observations and analyzed the data. GMRQ supported seashore observations, analyzed the data, and helped in their interpretation. All authors read and approved the final manuscript.

Funding

This work was partly supported by a Japan Society for the Promotion of Science KAKENHI Grant 17H04579, JP22H05207 and by the Japan Science and Technology Agency, AIPTrilateral AI Research Grant Number JPMJCR20G5.

Availability of data and materials

The logger data supporting the conclusions of this article are available at https://www.jamstec.go.jp/goorc/data/peru_smasuda. The buoy data are available at https://www.pmel.noaa.gov/gtmba/pmel-theme/pacific-ocean-tao.

Declarations

Competing interests

The authors declare that they have no competing interest.

Received: 25 July 2022 Accepted: 7 July 2023
Published online: 17 July 2023

References

Chavez FP, Messié M (2009) A comparison of eastern boundary upwelling ecosystems. Prog Oceanogr 83:80–96. https://doi.org/10.1016/j.pocean.2009.07.032

Chavez FP, Strutton PG, McPhaden MJ (1998) Biological-physical coupling in the central equatorial Pacific during the onset of the 1997–98 El Niño. Geophys Res Lett 25:3543–3546. https://doi.org/10.1029/98GL02729

Chelton DB, Davis RE (1982) Monthly mean sea-level variability along the west coast of North America. J Phys Oceanogr 12:757–784

Clarke AJ (1992) Low frequency reflection from a non-meridional eastern ocean boundary and the use of coastal sea level to monitor eastern Pacific equatorial Kelvin waves. J Phys Oceanogr 22:163–183. https://doi.org/10.1175/1520-0485(1992)022%3c0163:LFRFAN%3e2.0.CO;2

Cravatte S, Picaut J, Eldin G (2003) Second and first baroclinic Kelvin modes in the equatorial Pacific at intraseasonal time scales. J Geophys Res 108:3266. https://doi.org/10.1029/2002JC001511

Dewitte B, Purca S, Illig S, Renault L, Giese B (2008) Low frequency modulation of the intra-seasonal equatorial Kelvin wave activity in the Pacific Ocean from SODA: 1958–2001. J Clim 21:6060–6069

Espinoza-Morriberón D, Echevin V, Colas F, Tam J, Gutierrez D, Graco M, Ledesma J, Quispe-Ccalluari C (2019) Oxygen variability during ENSO in the Tropical South Eastern Pacific. Front Mar Sci 5:1–20. https://doi.org/10.3389/fmars.2018.00526

Fiedler PC, Talley LD (2006) Hydrography of the eastern tropical Pacific: a review. Prog Oceanogr 69:143–180. https://doi.org/10.1016/j105.pocean.2006.03.008

Goddard L, Philander S-G (2000) The energetics of El Niño and La Niña. J Clim 13:1496–1516

Good SA, Martin MJ, Rayner NA (2013) EN4: quality controlled ocean temperature and salinity profiles and monthly objective analyses with uncertainty estimates. J Geophys Res 118:6704–6716. https://doi.org/10.1002/2013JC009067

Grados C, Chaigneau A, Echevin V, Domínguez N (2018) Upper ocean hydrology of the Northern Humboldt current system at seasonal, interannual and interdecadal scales. Prog Oceanogr 165:123–144. https://doi.org/10.1016/j.pocean.2018.05.005

Gronell A, Wijffels SE (2008) A semiautomated approach for quality controlling large historical ocean temperature archives. J Atmos Ocean Technol 25:990–1003. https://doi.org/10.1175/JTECHO539.1

Guinehut S, Coatanoan C, Dhomps A-L, Traon P-YL, Larnicol G (2009) On the use of satellite altimeter data in Argo quality control. J Atmos Ocean Technol 26:395–402. https://doi.org/10.1175/2008JTECHO648.1

IMARPE (2020) Situacion del stock norte-centro de la anchoveta peruana (Engraulis ringens) al mes de mayo de 2020 y perspectivas de

explotacion para la primera temporada de pesca del año. Reporte tecnico Oficio N.330-2020-IMARPE, pp 1–57. http://www.imarpe.gob.pe/imarpe/descarga_informe.php?archivo=107 (in Spanish)
Ingleby B, Huddleston M (2007) Quality control of ocean temperature and salinity profiles-Historical and real-time data. J Mar Syst 65:158–175. https://doi.org/10.1016/j.jmarsys.2005.11.019
Jigena-Antelo B, Estrada-Ludeña C, Howden S, Rey W, Paz-Acosta J, Lopez-García P, SalazarRodriguez E, Endrina N, Muñoz-Pérez JJ (2023) Evidence of sea level rise at the Peruvian Coast (1942–2019). Sci Total Environ 859:160082. https://aquila.usm.edu/fac_pubs/20517
Johnson GC, Sloyan BM, Kessler WS, McTaggart KE (2002) Direct measurements of upper ocean currents and water properties across the tropical Pacific during the 1990s. Prog Oceanogr 52:31–61. https://doi.org/10.1016/S0079-6611(02)00021-6
Johnson GC, Hosoda S, Jayne SR, Oke PR, Riser SC, Roemmich D, Suga T, Thierry V, Wijffels SE, Xu J (2022) Argo-two decades: global oceanography, revolutionized. Ann Rev Mar Sci 14:379–403
Kovats R-S, Bouma M-J, Hajat S, Worrall E, Haines A (2003) El Niño and health. The Lancet 362:1481–1489
Kuntz LB, Schrag DP (2018) Hemispheric asymmetry in the ventilated thermocline of the tropical Pacific. J Clim 31:1281–1288. https://doi.org/10.1175/JCLI-D-17-0686.1
Lukas R (1986) The termination of the equatorial undercurrent in the eastern Pacific. Prog Oceanogr 16:63–90. https://doi.org/10.1016/0079-6611(86)90007-8
McPhaden MJ, Hayes SP (1989) Moored observations of the Pacific north equatorial countercurrent. Eos Trans Am Geophys Union 70:1148
McPhaden MJ, Yu X (1999) Equatorial waves and the 1997–98 El Niño. Geophys Res Lett 26:2961–2964. https://doi.org/10.1029/1999GL004901
McPhaden MJ, Santoso A, Cai W (2019) Understanding ENSO in a charging climate. Eos Trans Am Geophys Union. https://doi.org/10.1029/2019EO124159
Montes I, Colas F, Capet X, Schneider W (2010) On the pathways of the equatorial subsurface currents in the eastern equatorial Pacific and their contributions to the Peru-Chile Undercurrent. J Geophys Res Oceans 115:1–16. https://doi.org/10.1029/2009JC005710
Philander S-G (2004) Our affair with El Niño: how we transformed an enchanting Peruvian current into a global climate hazard. Princeton Univ Press, Princeton
Qin X, Menviel L, Sen Gupta A, van Sebille E (2016) Iron sources and pathways into the Pacific Equatorial Undercurrent. Geophys Res Lett 43:9843–9851. https://doi.org/10.1002/2016GL070501
Roemmich D, Gilson J (2009) The 2004–2008 mean and annual cycle of temperature, salinity, and steric height in the global ocean from the Argo Program. Prog Oceanogr 82:81–100
Rosales Quintana GM, Marsh R, Icochea Salas LA (2021) Interannual variability in contributions of the Equatorial Undercurrent (EUC) to Peruvian upwelling source water. Ocean Sci 17:1385–1402. https://doi.org/10.5194/os-17-1385-2021
Santos F, Gómez-Gesteira M, deCastro M, Álvarez I (2012) Variability of coastal and ocean water temperature in the upper 700 m along the Western Iberian Peninsula from 1975 to 2006. PLoS ONE 7:e50666. https://doi.org/10.1371/journal.pone.0050666
Thompson RORY (1982) Low-pass filters to suppress inertial and tidal frequencies. J Phys Oceanogr 13:1077–1108

Publisher's Note